52nd AAVLD Diagnostic Pathology Slide Session

American Association of Veterinary Laboratory Diagnosticians

San Diego, California
Saturday, October 10, 2009
3:30-6:00 PM

52nd AAVLD Diagnostic Pathology Slide Session
October 14, 2009 San Diego, CA

Case #	Slide label	Presenter	Species
1	ADDL	Ramos-Vara	Llama
2	ADDL	Frank	Llama
3		Cooley	Ox
4	ADDL	Jennings	Ox
5		Moore	Horse
6	VMDL-MO	Johnson	Horse
7	9050173	Smith	Horse
8		Scholes	Pig
9	ADDL	Durkes	Coyote
10	KSVDL	Janardhan	Dog
11	OK ADDL	Cramer	Dog
12	MSU DCPAH	Desjardins	Dog
13	ADDL	Burcham	Dog
14		Kiupel	Bearded dragon
15		Roberts	Snake
16		Evely	Piranha
17	S0902746 F1	Uzal	Rabbit
18	VMDL-MO	Johnson	Dog

52nd AAVLD Diagnostic Pathology Slide Session

October 14, 2009 San Diego, CA

Case #	Presenter	Species	Diagnosis
1	Ramos-Vara	Llama	Ocular coccidiodomycosis
2	Frank	Llama	Parelaphostrongylosis, spinal cord
3	Cooley	Ox	Ameloblastic fibro-odontoma
4	Jennings	Ox	BoHV-1 encephalitis
5	Moore	Horse	Osteomyelitis
6	Johnson	Horse	Neuromas
7	Smith	Horse	Eosinophilic enteritis
8	Scholes	Pig	Ganglioneuromas
9	Durkes	Coyote	Pulmonary paragonimiasis
10	Janardhan	Dog	Squamous cell carcinoma
11	Cramer	Dog	Xanthogranuloma
12	Desjardins	Dog	Exfoliative lupus erythematosus
13	Burcham	Dog	Thyroiditis
14	Kiupel	Bearded dragon	Somastotatinoma
15	Roberts	Snake	Sarcocystosis
16	Evely	Piranha	Ocular mycobacteriosis
17	Uzal	Rabbit	Enteric clostridiosis
18	Johnson	Dog	*Encephalitozoon* encephalitis

Ocular coccidioidomycosis in a llama (*Lama glama*)

***J.A. Ramos-Vara**, M. Coster, and R. Vemulapali*
Animal Disease Diagnostic Laboratory and Department of Comparative Pathobiology (Ramos, Vemulapali); Department of Veterinary Clinical Sciences (Coster), Purdue University, West Lafayette, IN

A 7-year-old, male llama was referred to the Purdue University VTH with a 3-month history of epiphora and blepharospasm of the right eye. Clinical diagnoses were nonulcerative keratitis, corneal stromal abscessation, and active, chronic anterior uveitis. Gross examination of the affected eye revealed multiple white nodules expanding the iris, ciliary body and cornea. Histologically, the iris, ciliary body and cornea had multiple distinct granulomas, each with a central area of necrosis or neutrophilic infiltrate surrounded by epithelioid macrophages and lymphocytes. Mild fibrosis surrounded some of the granulomas. Within the center of many granulomas and sometimes throughout their diameter were numerous 40 to 90 µm in diameter fungal spherules with a thick, refractile wall; some spherules contained numerous ovoid to round 2 to 7 µm in diameter structures interpreted as endospores. The filtration angle associated with the affected iris was closed. A diagnosis of coccidioidomycosis was confirmed by PCR as *C. posadasii* by sequence analysis of the GAC microsatellite locus.

Coccidioidomycosis in the USA is geographically confined to southwest states. *Coccidioides immitis* is the classically described California strain, and *C. posadasii* is the non-California strain. Although the llama of this report was located in Indiana, it had previously resided in Idaho. Exposure up to 3 years before disease onset has been reported in canine coccidioidomycosis. Systemic coccidioidomycosis in domestic animals includes respiratory, dermatologic, musculoskeletal, neurologic, and ophthalmologic manifestations. Ocular manifestations of coccidioidomycosis are typically considered to be secondary to hematologic spread following primary respiratory tract infection. Clinical evidence of systemic coccidioidomycosis in this llama was apparent 9 months after the diagnosis of keratouveitis. Necropsy performed revealed multisystemic granulomatous disease including the skin, lymph nodes, lungs, heart, liver, kidney, and spleen.

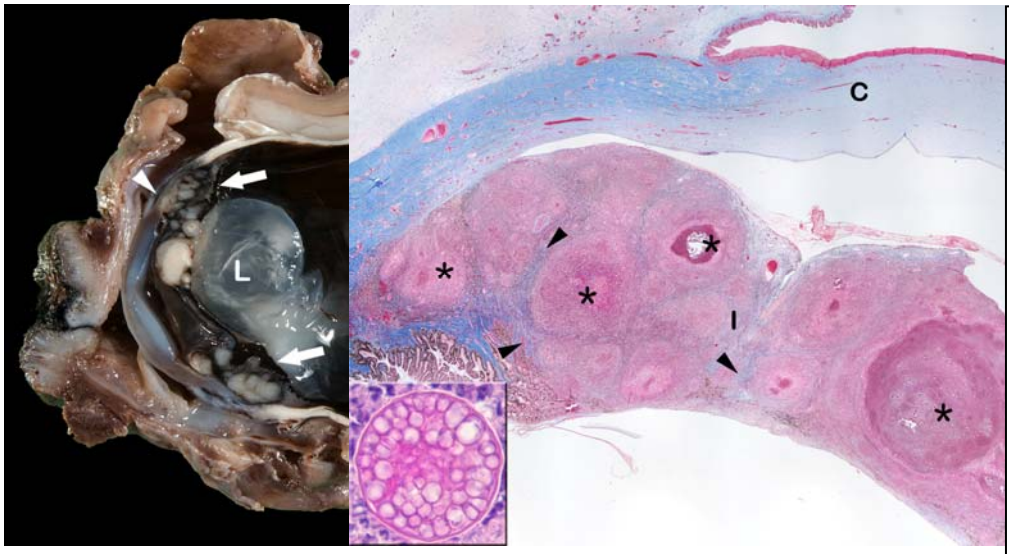

Fig. 1. Anterior portion of the globe showing granulomas in the iris (arrows) and corneal edema (arrowhead). L = Lens.
Fig. 2. Masson trichrome stain. C = Cornea. I = Iris. Asterisk = Granuloma. Arrowhead = Fibrosis. Inset = *Coccidioides* spherule

Parelaphostrongylus tenuis infection in a llama (*Lama glama*)

Chad Frank, *Pam Mouser, Jordan Hammer, Michel Lévy*
Animal Disease Diagnostic Laboratory-Department of Comparative Pathobiology (Frank, Mouser) and Veterinary Animal Clinical Sciences (Hammer, Lévy), Purdue University, West Lafayette, IN

A 2.5 year old female llama was submitted to Purdue University Animal Disease Diagnostic Laboratory for necropsy. Reportedly, the llama had a two week history of dragging the left pelvic limb. The clinical signs progressed to tetraparesis and loss of superficial pain in the rear limbs. Evaluation of a sample of cerebrospinal fluid revealed an elevated protein content and an increased white blood cell count (110/μL, Ref. Range < 5) with a predominance of eosinophils (78%). At necropsy, the white matter of the thoracic spinal cord contained a poorly demarcated, pale red to brown focus, measuring 3 mm in diameter. Microscopic lesions were predominantly restricted to the white matter from the caudocervical to lumbar spinal cord. There was multifocal necrosis of the white matter; adjacent myelin sheaths were dilated with either centrally-located swollen hypereosinophilic axons (spheroids) or empty spaces. These regions were infiltrated by low to moderate numbers of gitter cells, reactive astrocytes, and fewer multinucleated giant cells. Numerous (15-20) longitudinal and cross sections of nematode parasites were present in the affected regions. The parasites ranged in size from 100 to 150 um in diameter; they had a thin cuticle with a smooth surface, prominent accessory hypodermal chords, a thin rim of polymyarian coelomyarian musculature, intestines lined by a few multinucleated cells, and occasional gonads, consistent with adult and larval *Parelaphostrongylus spp*.

Parelaphostrongylus tenuis has an indirect life-cycle that involves definitive and intermediate hosts, the white tail deer and snail or slug, respectively. Adult nematodes occupy subdural spaces and cranial venous sinuses of the definitive host's central nervous system. The life cycle is initiated by the release of eggs into venous circulation. The eggs travel to the heart, then to the lungs where first stage larvae hatch and enter alveolar spaces. First stage larvae are coughed up, swallowed, and eventually passed in feces. Once in the environment, L1 larvae penetrate or are ingested by an intermediate host and, over a 3 to 4 week period, undergo two molts to emerge as infective third stage larvae. The life cycle is propagated by accidental ingestion of the infected intermediate host by white tail deer or an aberrant host. Following ingestion, L3 larvae migrate through the abomasum (or C3) and peritoneal cavity, enter the spinal cord via spinal nerve roots and mature in the dorsal horn of the spinal cord gray matter. From here, mature adults typically migrate to and reside in subdural spaces, uneventfully. Alternatively, the life cycle of the parasite is altered in aberrant hosts, resulting in the migration of L3 larvae through the spinal cord. Interestingly, in this case of aberrant host-parasite migration, *P. tenuis* adult nematodes were present alongside immature larvae in the spinal cord.

The clinical signs (see above) localized the lesions to the cervical and thoracolumbar spinal cord. This localization was consistent with the areas of heavier worm burdens and more severe white matter damage, microscopically.

References:

1. Lankester MW: Extrapulmonary lungworm of cervids, 2001. In *Parasitic Diseases of Wild Mammal.* Samuel WM, Pybus MJ, Kocan AA Eds, Iowa State University Press, Ames, IA. pp 228-246.
2. Summers BA, Cummings JF, Lahunta AD: 1995. Veterinary neuropathology. Mosby, St. Louis, MO. pp 159-161.

Rostral mandibular mass in a 7-year-old Brangus cow

***A.J. Cooley**, B.S. Baughman, M.W. Thomas, S.A. Fleming*
Department of Pathobiology & Population Medicine (Cooley, Baughman, Fleming) and Department of Clinical Sciences (Thomas), College of Veterinary Medicine, Mississippi State University, MS

A prominent bulge was noted on the rostral mandible of a 7-year-old Brangus cow. Progressive growth had been noted over approximately 4 months. Radiographs revealed an expansile destructive mass with numerous interspersed amorphous mineral opacities suggestive of neoplasia. A definitive biopsy diagnosis was made, but the cow was euthanized.

The mass was 13x10x8cm and replaced or displaced incisors. Cut surface revealed white translucent tissue with interspersed 2-4mm bony foci. The tumor was discretely localized and had superficial zones of necrosis and ulceration. Histologically, irregular sometimes interconnecting lobules and cords of loosely arrayed cells interpreted as odontogenic epithelium were marginated by palisades of columnar epithelium in single layers. Intervening tissue consisted of a loose mesenchymal stroma resembling dental pulp. Rarely, the columnar palisades were immediately adjacent to an eosinophilic matrix that was occasionally mineralized that was reminiscent of enamel. Degenerating columnar palisades were sometimes adjacent to eosinophilic material with the suggestion of fine radiating tubules (dentin). The dentin like material with radiating tubules was associated with trabeculae of bone. The mesenchymal matrix identified as dental pulp stained positively with vimentin on immunohistochemistry. The loosely arrayed cells marginated by palisades of columnar epithelium stained positively with cytokeratin, consistent with odontogenic epithelium. A diagnosis of ameloblastic fibro-odontoma was made. Even though this tumor is rare in all species, this is the most common odontogenic neoplasm in cattle. These tumors are more common in young cattle and site of predilection is the anterior mandible. In a review of ameloblastic fibromas and related tumors in cattle, animals ranged from newborn to 2.5 years. This cow is an exception with respect to age. The tumors are localized and do not metastasize. Osteolysis of the jaw and interference with mastication are a common consequence.

Reference:

Gardner DG: 1996, Ameloblastic fibromas and related tumors in cattle. Journal of Oral Pathology & Medicine 25: 119-124.

Bovine herpesvirus-1 associated necrotizing encephalitis in an Angus steer

Ryan N. Jennings, *Roman M. Pogranichniy, and José Ramos-Vara*
Animal Disease Diagnostic Laboratory and Department of Comparative Pathobiology, Purdue University, West Lafayette, Indiana

A one-month-old Angus crossbred steer, recently vaccinated for BoHV-1 with a modified live virus, was submitted to the Animal Disease Diagnostic Laboratory for necropsy. The history indicated an acute onset and rapid progression of neurologic signs consisting of circling, walking backwards, vocalizing, blindness, opisthotonus, and death within twelve hours of onset.

Grossly, the calvarium contained increased cerebrospinal fluid. The rostral frontal cortices of the right and left cerebral hemispheres each contained a focal, slightly raised, moderately well-demarcated, 4 mm to 1 cm in diameter dark red foci that extended into the subjacent brain parenchyma. A tentative diagnosis of *Histophilus somni*-associated encephalitis was made.

Microscopically, the rostral cerebral cortical gray matter contained multiple moderately well-demarcated foci of necrosis and hemorrhage. The necrotic foci were composed of abundant hemorrhage interspersed with moderate numbers of glial cells and few histiocytes and neutrophils. The adjacent gray matter contained degenerate neurons and was infiltrated by numerous glial cells, composed predominantly of astrocytes with large vesicular nuclei and abundant eosinophilic cytoplasm, and fewer lymphocytes, plasma cells, histiocytes, and neutrophils. Few neurons adjacent to the necrotic foci had marginated chromatin and contained round to polyhedral eosinophilic intranuclear inclusions.

The histologic lesions were consistent with necrotizing encephalitis. The intranuclear viral inclusions found within degenerate neurons were suspected to be herpesviral inclusions. Bovine herpesvirus was isolated from brain tissue and confirmed to be BoHV-1 by fluorescent antibody testing of the isolate and negative for BoHV-2, 4, and 5. Degenerate neurons within and surrounding the necrotic foci showed positive cytoplasmic immunohistochemical labeling for BoHV-1 antigen, confirming a diagnosis of BoHV-1-associated necrotizing encephalitis.

Bovine herpesviral necrotizing meningoencephalitis is an uncommon and sporadic form of herpesvirus infection in calves, and rarely adult cattle. Reports of herpesviral meningoencephalitis in calves are predominantly associated with bovine herpesvirus-5, and less commonly bovine herpesvirus-1. The majority of case reports of natural BoHV-1 and BoHV-5 meningoencephalitis are from South America. Although the encephalitis in this calf included a small population of neutrophils, the classic histologic feature is a nonsuppurative necrotizing meningoencephalitis that is predominantly focused on the rostral cerebrum, thalamus, and occasionally the cerebellum. BoHV-1 should be considered as a potential etiology for necrotizing encephalitis in calves.

References:

Maxie and Youssef. Nervous System. In: *Jubb, Kennedy, and Palmer's Pathology of Domestic Animals 5th edition.* Maxie (2007). Rissi DR, Pierezan F, Lombardo de Barros CS. Neurological disease in cattle in southern Brazil associated with bovine herpesvirus infection. J Vet Diagn Invest; 20:346-9 (2008).

Osteomyelitis in a foal

Ian N. Moore
Diagnostic Center for Population and Animal Health, Michigan State University, Lansing MI 48910/ National Institutes of Health, National Cancer Institute, Bethesda Maryland 20892

A 3-month-old, male, equine quarter horse was euthanized and submitted to the Diagnostic Center for Population and Animal Health following 3-4 weeks history of left forelimb lameness, progressive ataxia and decreased mobility of the neck to the left side. Prior to postmortem examination, the animal's cervical region was evaluated radiographically and via computed tomography. A 3-demensional reconstruction of the animal's cervical region (C1-C3) was also generated. These images allowed greater antemortem visualization of the affected cervical segments. During postmortem evaluation, the cervical region was carefully dissected and revealed necrosis of the left occipital condyle and corresponding atlas articulation (atlanto-occipital joint). The affected areas were devoid of articular cartilage, irregularly shaped, pale tan yellow, and extremely friable. These necrotic regions corresponded with the defects observed with computed tomography and reconstructed images. The controlateral articulations were grossly within normal limits. Histologically, the affected bone was characterized by severe suppurative inflammation, osteonecrosis, fibrosis, and prominent bone remodeling. The corresponding spinal cord segments were markedly inflamed and contained areas of necrosis. The contralateral atlanto-occipital joint was also examined histologically and was within normal histological limits. This animal had also prior clinical history of low IgG (consistent with failure of passive transfer), septic arthritis, and a guttural pouch infection; *Streptococcus zooepidemicus* was isolated.

Neuromas associated with bilateral repeated neurectomy and exunguilation in a horse

Gayle C. Johnson
Veterinary Medical Diagnostic Laboratory and the Department of Veterinary Pathobiology, College of Veterinary Medicine, University of Missouri, Columbia, MO 65211

A 3 year old Quarter horse mare, purchased as a show horse, underwent repeated bilateral digital neurectomies at the hands of her trainer. The third surgery removed the nerve bilaterally dorsal to the fetlock joint, a level consistent with ablation of both branches of the digital nerve and complete denervation of the foot. The mare was euthanized because of acute sloughing of the right front hoof, followed by rotation of the third phalanx on the left front foot. Considerable connective tissue adhered the dermis to underlying soft tissues at all surgical sites, but especially on the right. All of P3 (which had luxated) and the distal end of P2 on the right were dull and gray-brown externally and internally. The medial and lateral digital nerves could be traced only to a point 2-3 cm proximal to the fetlock joint on both legs, where they terminated in round firm bulbous structures and were buried in the connective tissue of the leg. The medial right digital artery was not observed grossly but was present microscopically, and all other digital arteries were seen grossly. Histologically there was increased mature fibrous tissue around the nerves and vessels, and the nerves terminated distally in a ball of intertwined fibers depleted of axons. There was progressive reduction in the number and diameter of axons in the nerves from proximal to distal in the samples examined histologically. Fibrosis and neuroma formation were less marked on the right foreleg. Tyrosine hydroxylase immunohistochemistry demonstrated autonomic fibers in tissue from the left but not the right legs.

Published estimates of neuroma formation following digital neurectomy in horses vary from 1-25%. Loss of the hoof wall is an uncommon complication, and is associated with recurrent surgeries such as occurred in this case. It is not clear whether the artery was damaged during one of the surgeries and ischemia is the mechanism of exunguilation, or whether diminished autonomic supply to the vessels of the hoof might be responsible for abnormal vasoregulation and separation of the laminae. Published opinion regarding the matter suggests that excessive scarring around the vasculature is the most likely cause of hoof loss following this surgery.

References:

1. Evans,L.H. (1975) Complications other than painful neuromas following posterior digital neurectomy. *Arch Amer College Vet Surg* **4**(2):20-22, 1975.
2. Keller, H. (1969) [Sequelae of neurectomy of the volar nerves in horses: neuromas, regeneration, and reinnervation of nerve stumps] *Berl Munch Tierarztl Wochenschr* **82**(13): 244-247.

Idiopathic focal eosinophilic enteritis in a horse

Steve Smith, *Brad Njaa*

Center for Veterinary Health Sciences, Oklahoma State University, Stillwater, OK

A 14-year-old Quarter Horse mare presented to the OSU veterinary medical teaching hospital with an 18 hour history of moderate colic. Two to three years prior, the mare had experienced another bout of colic that resolved with medical treatment. On physical examination, reflux dripped from the nose, and rectal palpation revealed segmental distension of the small intestine. Surgery revealed a mid-jejunal stricture with fluid distension and feed material proximal to the stricture. An intestinal resection and anastomosis was performed, and sections of the affected bowel were submitted for biopsy.

On histologic examination, the wall of the small intestine was markedly thickened by severe inflammation and fibrous connective tissue that primarily infiltrated the submucosa and the muscularis externa. Inflammatory cells consisted predominantly of eosinophils, with smaller numbers of lymphocytes and macrophages. There was also regionally extensive submucosal edema and dilation of lymphatics. The overlying intestinal mucosa was essentially normal.

Idiopathic focal eosinophilic enteritis with fibrosis has been previously described in horses as a cause of focal stricture formation, but it is uncommonly reported. Affected animals typically have thickened serosal plaques or circumferential constrictions of the small intestine, have no evidence of gastrointestinal parasitism, and may present with small intestinal obstruction. The histologic lesions consist of transmural eosinophilic enteritis, edema, and fibrosis. A specific underlying cause is not known, although changes in management and dietary factors have been discussed. This disease is thought to be a specific, localized form of equine inflammatory bowel disease. In most of the reported cases, surgical excision of the affected region of small intestine is curative.

References:

1. Archer DC, Barrie Edwards G, Kelly DF, French NP, Proudman CJ: Obstruction of equine small intestine associated with focal idiopathic eosinophilic enteritis: an emerging disease? Veterinary journal (London, England **171:** 504-512, 2006
2. Makinen PE, Archer DC, Baptiste KE, Malbon A, Proudman CJ, Kipar A: Characterisation of the inflammatory reaction in equine idiopathic focal eosinophilic enteritis and diffuse eosinophilic enteritis. Equine veterinary journal **40:** 386-392, 2008
3. Southwood LL, Kawcak CE, Trotter GW, Stashak TS, Frisbie DD: Idiopathic focal eosinophilic enteritis associated with small intestinal obstruction in 6 horses. Veterinary surgery **29:** 415-419, 2000
4. Swain JM, Licka T, Rhind SM, Hudson NP: Multifocal eosinophilic enteritis associated with a small intestinal obstruction in a standardbred horse. The Veterinary record **152:** 648-651, 2003

Multiple intestinal ganglioneuroblastomas in a 17-week-old Large White gilt

***Scholes SFE**, Wessels ME, Reichel R, Gaudie CM*
VLA Lasswade, Midlothian, EH26 0PZ Scotland (Scholes); VLA Preston, Lancashire PR3 5HE (Wessels) VLA Thirsk, North Yorkshire YO7 1PZ (Reichel, Gaudie)

One pig was submitted for investigation of illthrift in grower pigs. Necropsy observations included poor body condition, stomach empty with variable hyperkeratosis of oesophageal inlet, and multiple moderately well demarcated jejunal masses visible on the serosal aspect (fig 1, arrows). Cut surfaces of these masses revealed purplish soft expansions of the intestinal wall bulging into the lumen (maximum dimension 2.5cm). Additional observations were 5 small intestinal intussusceptions (fig 1, crosses), 2 of which involved necrosis of the bowel wall, and marked distension of the duodenum and anterior jejunum with brown watery luminal content.

Two intestinal masses were examined histopathologically. They consisted of moderately well demarcated connecting nests of neoplastic cells that effaced mural architecture particularly of mucosa and submucosa. Towards the luminal aspect, cells with medium - large open nuclei and abundant cytoplasm were interspersed with cells with much smaller condensed nuclei and finely fibrillar eosinophilic tract-like areas with few nuclei. Crypts in adjacent mucosa were markedly hyperplastic. Towards the outer aspect, neoplastic cells had smaller nuclei and tended to be more closely spaced, often pallisading around the outer aspect of nests and columns of cells, with prominent intervening areas containing few nuclei. Immunostaining for neurofilament (NF) revealed neuronal morphology of larger cells and of abundant fine neurites in fibrillary areas (Fig 2, labelled brown) but less labelling of cells in outer areas. Glial fibrillary acidic protein (GFAP) labelled a different population of smaller cells (Fig 2, labelled red) often peripherally located within nests of neoplastic cells. Synaptophysin immunohistochemistry revealed extensive punctate labelling particularly of fibrillary tracts.

The anatomical locations and the histological and immunohistochemical observations of populations of both atypical ganglion cells (NF+) and non-neuronal supporting glial-type cells (GFAP+) indicate neural neoplasms originating from enteric ganglia. Ganglioneuroblastoma would appear to be an appropriate designation in view of the limited neuronal differentiation, for example the paucity of Nissl substance. This is in contrast to a previous report of multiple enteric ganglioneuromas in a sow in which clusters of well differentiated cells resembling enteric neurones were surrounded by tissue resembling normal nerve fibre tracts. Presence of crypt hyperplasia and multiple intussusceptions suggest neurosecretory activity of neoplastic cells with effects on epithelial kinetics and intestinal motility.

Reference

Multiple ganglioneuroma derived from intramural plexus of jejunum in a sow.
Une Y *et al*. Jpn J Vet Sci (1984) **46** 247-250


FIG 1

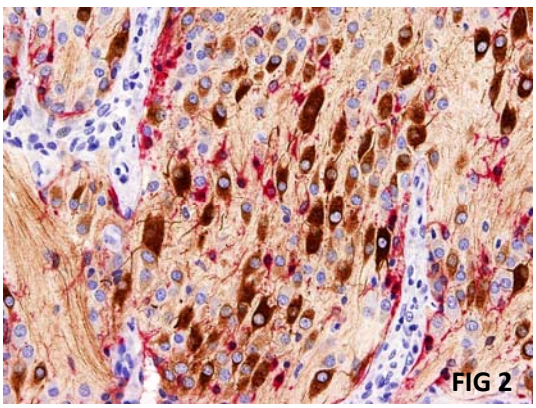
FIG 2

Granulomatous pneumonia in a coyote caused by *Paragonimus kellicotti*

A. Durkes *and T. Lin*
Animal Disease Diagnostic Laboratory and Department of Comparative Pathobiology, Purdue University, West Lafayette, IN

An adult female coyote (*Canis latrans)* of unknown age was found dead on the side of the road. Postmortem examination of the coyote revealed the animal was thin with little subcutaneous or abdominal adipose tissue. A gunshot through the thoracic cavity had fractured the right and left cranial lung lobes, esophagus, and trachea. The right middle and caudal lung lobes, and the left caudal lung lobe contained multifocal to coalescing areas of firm, approximately 3 cm in largest diameter, mottled dark red to black nodules. On cut section, the nodules were mottled dark red and tan and contained multiple cystic areas lined with a thick fibrous capsule. Within a number of capsules were tan, ellipsoid, flukes measuring approximately 0.6 cm – 1.0 cm in length and 0.2 -0.4 cm in width. Histologically, the grossly observed pulmonary trematodes were in the pulmonary parenchyma and characterized by a spiny tegument, lack of coelom, muscular anterior sucker, paired ceca and peripherally located vitellaria containing eosinophilic globules. Adult trematodes were histologically consistent with *Paragonimus kellicotti.* A thick fibrous capsule surrounded each trematode. Bronchioles and alveoli adjacent to the fibrous capsule were disrupted and filled with numerous epithelioid macrophages with fewer neutrophils, eosinophils and lymphocytes. The bronchiolar epithelium was necrotic. Alveolar septa were multifocally necrotic with loss of cell outlines, karyorrhexis, and karyolysis. Many trematode eggs, approximately 90 microns in length and 50 microns in diameter, with thick, refractile, golden brown walls and an operculum were randomly scattered in the pulmonary parenchyma and surrounded by numerous inflammatory cells, primarily epithelioid macrophages, eosinophils, and neutrophils. *Paragonimus kellicotti* eggs were recovered by fecal sedimentation and confirmed by parasitology.

Paragonimus kellicotti, classified as a Digenetic Trematode, is a lung fluke of wild and domestic carnivores and is widespread in eastern and southern North America. The life cycle of *P. kellicotti,* like all digenetic Trematodes, is indirect involving an aquatic snail (*Pomotiopsis* sp.) as the intermediate hose, then crayfish or freshwater crabs as the second intermediate host. More specifically, a miracidium from a hatched trematode egg enters an aquatic snail and beomes a sporocyst which gives rise to rediae. Each rediae gives rise to daughter rediae. Each daughter redia gives rise to several cercariae which escape from the snail and encyst in the second intermediate host as metacercariae. The definitive host ingests the metacercariae-laden secondary intermediate host and completes the life cycle. Clinical signs of *P. kellicotti* pulmonary infection include chronic cough, dyspnea, exercise intolerance, salivation, gagging, haemoptysis, depression, anorexia, and weight loss. Antemortem diagnosis requires fecal sedimentation or direct smear to identify characteristic trematode eggs. Postmortem diagnosis is accomplished by identification of pulmonary Trematodes and associated lesions.

References:

Presidente, J. and R. Ramsden (1975). "*Paragonimus kellicotti* infection in wild carnivores in southwestern Ontario: II. Histopathologic features." Journal of Wildlife Diseases 11: 364-375.

Ramsden, R. and J. Presidente (1975). "*Paragonimus kellicotti* infection in wild carnivores in southwestern Ontario: I. Prevalence and gross pathologic features." Journal of Wildlife Diseases 1975: 136-141.

Verrucous squamous cell carcinoma in the oral cavity of a dog

Kyathanahalli S. Janardhan
Diagnostic Medicine/Pathobiology, Kansas State University, Manhattan, Kansas

A five month-old Bull Mastiff puppy was presented to a veterinarian with a complaint of mass in the oral cavity. The mass was present on the ventral jaw between the second and the third premolar. The mass displaced the premolars and probably involved the underlying bone. The mass was surgically removed and submitted for histopathological evaluation. The tissue was routinely processed, sectioned and stained with hematoxylin and eosin.

Arising from the gingival mucosal epithelium was an exophytic, poorly-delineated neoplasm forming papillary projections lined by several layers of squamous epithelial cells. The basal portions of these projections were lined by basaloid cells. The cells had variably distinct borders, moderate to abundant amounts of eosinophilic cytoplasm and round nuclei containing coarsely stippled chromatin and prominent nucleoli. There was moderate anisocytosis and anisokaryosis. Several mitotic figures were present in the superficial layers. Scattered individually keratinized cells were present. The neoplastic cells in scattered locations infiltrated the surrounding connective tissue. Nests of neoplastic cells were present in the underlying alveolar bone. The surface was infiltrated by large numbers of neutrophils. The neoplasm was diagnosed as verrucous squamous cell carcinoma.

Verrucous squamous cell carcinoma also known as papillary squamous cell carcinoma is reported in both young and old dogs(*1, 2*). Because of only a few reports, not much is known about the biological behavior of this rare variant of squamous cell carcinoma. In two older dogs, the tumor recurred within 1-2 months and the dogs were euthanized(*1*). However, in one young dog, there was no recurrence at 2 years post-surgery(*2*). In humans the tumor is also known as verrucous carcinoma of Akermann and has been reported to occur most commnly in the oral cavity(*3, 4*). It is a slow growing, locally aggressive tumor with no reported metastasis(*3, 5*). It is strongly associated with tobacco, alcohol and human papillomavirus(*3*). In dogs the etiology is not known and is not associated with papillomavirus(*6*). Also, in the present case no papillomavirus was detected by immunohistochemistry. In humans surgical excision with wide margins is the treatment of choice and, radiation therapy is not preferred as it can transform the neoplasm into an anaplastic carcinoma(*4, 5, 7*). Although no such transformation of the neoplasm was observed in two dogs(*6*), studies involving large number of cases will be required to predict the behavior and treatment outcomes for this tumor in dogs.

References:

1. I. B. Van Rensburg, *J S Afr Vet Assoc* **53**, 209 (1982).
2. B. L. Stapleton, J. M. Barrus, *J Vet Dent* **13**, 65 (1996).
3. R. R. Walvekar *et al.*, *Oral Oncol* **45**, 47 (2009).
4. F. T. Kraus, C. Perezmesa, *Cancer* **19**, 26 (1966).
5. S. Jacobson, M. Shear, *J Oral Pathol* **1**, 66 (1972).
6. G. K. Ogilvie *et al.*, *J Am Vet Med Assoc* **192**, 933 (1988).
7. P. G. Arduino, M. Carrozzo, M. Pagano, S. Gandolfo, R. Broccoletti, *Minerva Stomatol* **57**, 335 (2008).

Suprasellar xanthogranuloma in a Standard Poodle

Sarah D. Cramer, *Jerry W. Ritchey, Emily Medici, Jill Brunker*
Department of Veterinary Pathobiology (Cramer, Ritchey), Boren Veterinary Medical Teaching Hospital (Brunker, Medici), Oklahoma State University, Stillwater, OK

Necropsy was performed on a 7 year old, castrated male Standard Poodle with a history of hypothyroidism and atypical Cushing's disease. Prior to euthanasia, the dog developed neurologic signs including proprioceptive deficits, ataxia, aggression, and equivocal seizures. Gross examination revealed a mass on the ventral surface of the brain that extended dorsally into the hypothalamus and ventrally into the sella turcica. The mass was 1.5 x 1.0 x 1.5 cm, green to brown, and had multiple, small cystic spaces that oozed thick, brown material. The pituitary gland was not identified grossly.

Histologically, the mass consisted of severe, xanthogranulomatous inflammation characterized by multinucleated giant cells, epithelioid macrophages, and abundant cholesterol clefts. Few, small, epithelial-lined ductular structures were scattered throughout the inflammation, and interspersed were many Rosenthal fibers. The overlying hypothalamic tissue was markedly rarefied. Examined sections did not contain identifiable pituitary tissue. A diagnosis of suprasellar xanthogranuloma was made based on histologic morphology.

Differential diagnoses include primary inflammation or inflammation secondary to degeneration or neoplasia. In humans, primary hypophysitis is rare and may be the result of autoimmune disease, while secondary hypophysitits may result from several systemic disease syndromes.[1] Primary hypophysitis has not been reported in the dog, but pituitary abcesses have been described in cattle.[2] Degenerative changes that may occur in this region of the brain include Rathke's cleft cysts,[3] or intra-arachnoid cysts,[7] both of which have been reported in dogs. Cyst rupture may have elicited inflammation.[4] Lastly, though there was not clear evidence of a neoplastic population, several canine neoplasms classically involve the suprasellar space, including pituitary adenomas, craniopharyngiomas[5] and suprasellar germ cell tumors.[6] The presence of bizarre astrocytic processes and Rosenthal fibers also raises the possibility of an astrocytoma.

References:

1 Cheung CC, Ezzat S, Smyth HS, Asa SL: The spectrum and significance of primary hypophysitis. J Clin Endocrinol Metab **86:** 1048-1053, 2001
2 Fernandes CG, Schild AL, Riet-Correa F, Baialardi CEG, Stigger AL: Pituitary abscess in young calves associated with the use of a controlled suckling device. Journal of Veterinary Diagnostic Investigation **12:** 70-71, 2000
3 Hasegawa D, Uchida K, Kobayashi M, Kuwabara T, Ide T, Ogawa F, Fujita M, Orima H: Imaging diagnosis-Rathke's cleft cyst Veterinary Radiology & Ultrasound **50:** 298-300, 2009
4 Murakami M, Nishioka H, Izawa H, Ikeda Y, Haraoka J: Granulomatous hypophysistis associated with rathke's cleft cyst: a case report. Minim Invasive Neurosurg **51:** 169-172, 2008
5 Neer TM, Reavis DU: Craniopharyngioma and associated central diabetes insipidus and hypothyroidism in a dog. Journal of the American Veterinary Medical Association **182:** 519-520, 1983
6 Valentine BA, Summers BA, Delahunta A, White CL, Kuhajda FP: Suprasellar germ-cell tumors in the dog-a report of 5 cases and review of the literature. Acta Neuropathologica **76:** 94-100, 1988

Exfoliative cutaneous lupus erythematosus in the German Short-haired Pointer

Danielle Desjardins *and Barbara Steficek*
Diagnostic Center for Population and Animal Health, Michigan State University, Lansing, MI

A 15-month-old German Short-haired Pointer presented to the VTH Small Animal Clinic of MSU for a six month history of progressive hair loss and scaling. At the time of presentation, the dog was mildly pruritic and had shown mild improvement with Malaseb® shampoo. Three skin biopsies were obtained and submitted for histopathology to the Diagnostic Center for Population and Animal Heath.

Histologically, all sections of haired skin were characterized by moderate, multifocal vacuolar degeneration of the basal keratinocyte layer of the epidermis, with occasional hypereosinophilic, shrunken basal cells with pyknotic nuclei (dyskeratosis). Similar vacuolar alterations also affected portions of the follicular epithelium. There was mild to moderate, basketweave to laminar orthokeratotic hyperkeratosis and mild parakeratosis. The superficial dermis had moderate pigmentary incontinence, mild edema, mildly dilated lymphatic vessels, and low numbers of perivascular plasma cells, lymphocytes and mast cells. Similar inflammatory cell populations were focally present in periadnexal regions. No sebaceous glands were observed throughout the sections. Anagen follicles were present in multiple sections. No infectious agents were observed on routine H&E stained sections. A Periodic acid-Schiff stain for fungal agents was negative. The morphologic diagnosis for the haired skin was: Moderate stratum basale vacuolar degeneration; parakeratosis/hyperkeratosis; mild superficial perivascular dermatitis; and, diffuse sebaceous gland atrophy.

The combined clinical history and microscopic findings were consistent with the condition exfoliative cutaneous lupus erythematosus (ECLE) of the German Short-haired Pointer. The pathogenesis of ECLE is poorly understood, but its exclusivity to the GSHP strongly suggests a hereditary basis. In a 2005 study, IgG deposition in the epidermal and follicular basement membranes was detected by direct immunofluorescence in 100 % (19/19) and 41% (7/17) of affected dogs, respectively.[1] Normal canine skin does not demonstrate such autoantibodies. The destruction of sebaceous glands is thought to be secondary to inflammation at the level of the basement membrane. Antiseborrheic baths and immunomodulatory therapy for dogs with ECLE have generally given poor results.[2] Differential diagnosis include sebaceous adenitis, systemic lupus erythematosus, and erythema multiforme.[3]

References:

1. Bryden SL, et al. Clinical, histopathological and immunological characteristics of exfoliative cutaneous lupus erythematosus in 25 German short-haired pointers. Veterinary Dermatology 2005; 16: 239-252.
2. Scott DW, Miller WH, Griffin CE, eds. Small Animal Dermatology, 6th edn. Philadelphia: W.B. Saunders, 2001: 948-949.
3. Gross TL, Ihrke PJ, Walder EJ, Affolter, VK, eds. Skin Diseases of the Dog and Cat, 2nd edn. Ames: Blackwell Science Ltd, 2005: 59-61.

Lymphocytic thyroiditis in a mixed-breed dog

Grant N. Burcham *and Pamela Mouser*
Animal Disease Diagnostic Laboratory and Department of Comparative Pathobiology,
Purdue University, West Lafayette, IN

A 4-year-old black and tan spayed-female mixed-breed dog was submitted to the Animal Disease Diagnostic Laboratory (ADDL) for necropsy. The dog died suddenly without preceding clinical signs. The cause of death was determined to be a round cell neoplasm that infiltrated the myocardium.

Bilaterally, the thyroid glands were partially effaced by multifocal to coalescing aggregates of lymphocytes and fewer plasma cells. Lymphocytes formed lymphoid follicles, with distinct, centrally-located germinal centers comprised of larger lymphoblastic lymphocytes, and a surrounding mantle zone. Several thyroid follicles were filled with sloughed thyroid follicular cells and lymphocytes; some follicles were collapsed and contained degenerate follicular cells and leukocytes in their lumens. Aggregates of plump, epithelioid follicular cells with abundant granular and eosinophilic cytoplasm (oncocytes) were also scattered throughout thyroid parenchyma. Multiple foci of hemorrhage were scattered throughout the thyroid glands; blood vessels were congested.

Lymphocytic thyroiditis is an autoimmue disease that leads to progressive infiltration and destruction of the thyroid glands, with the end result being loss of thyroid parenchyma and clinical hypothyroidism. In adult-onset hypothyroidism in dogs, at least 50% of cases are a result of autoimmune lymphocytic thyroiditis. The disease in dogs mirrors the disease in people, which is known as Hashimoto's disease. In people, the pathogenesis of autoimmune lymphocytic thyroiditis includes induction of both humoral and cellular immunity. Cytotoxic T-cells infiltrate and destroy thyroid follicular epithelium while B-cells produce anti-TSH receptor antibodies, which inhibit the action of TSH. Anti-thyroglobulin and anti-thyroid peroxidase antibodies are also produced, but are thought to be secondary to destruction of thyroid parenchyma. In dogs, autoantibodies to the TSH receptor, thyroid peroxidase, and thyroglobulin are also found. Histologically the disease in humans and dogs is similar. Lymphocytic thyroiditis is characterized by complete or partial effacement of the thyroid glands by lymphocytes, plasma cells, and macrophages, with formation of germinal centers. Lymphocytes infiltrate between the follicular epithelial cells and can fill the follicles. Thyroid follicles become atrophic and may be lined by plump epithelial cells with abundant, granular eosinophilic cytoplasm, consistent with oncocytes. Ultrastructurally these cells contain numerous mitochondria, and are thought to represent a metaplastic change of the thyroid follicular epithelium. With continued inflammation and destruction, affected thyroid gland is replaced by fibrous connective tissue and dogs develop clinically-apparent hypothyroidism. The provided tissue represents a good example of an early case of lymphocytic thyroiditis in a dog.

References:

Capen. Endocrine glands. In: Jubb, Kennedy and Palmer's Pathology of Domestic Animals. 5th ed. Maxi (2007)
Graham et al. Etiopathologic findings of canine hypothyroidism. Vet Clin NA July 2007
Maitra and Kumar. The endocrine system. In: Robbibs Basic Pathology. 7th ed. Kumar, Cotran, and Robbins (2003)

Malignant somatostatinoma in a bearded dragon

***Matti Kiupel**, Jana M. Ritter, Michael M. Garner*
Diagnostic Center for Population and Animal Health, Michigan State University, E. Lansing, MI (Kiupel and Ritter); Northwest ZooPath, Monroe, WA (Garner)

A 2-year-old female bearded dragon (*Pogona vitticeps*) with a history of anorexia, weight loss, and severe hyperglycemia was submitted for necropsy. Neoplastic masses were identified in stomach and liver. The stomach mass presented as a single, discrete, well-circumscribed, pale tan to white, firm, 3 cm diameter nodule that protruded into the gastric lumen, causing ulceration of the gastric mucosa. Multiple smaller 0.5-1.0 cm in diameter discrete, sharply demarcated white nodules were observed throughout the hepatic parenchyma. Histologic examination revealed a neuroendocrine neoplasm within the gastric submucosa and suspected metastases within the liver. The gastric neoplasm was located primarily within and expanded the gastric submucosa. There was infiltration of neoplastic cells into the overlying mucosa and the underlying tunica muscularis, as well as infiltration of submucosal veins and lymphatics. Neoplastic cells of gastric and hepatic masses were similar morphologically. Cells were arranged in packets and trabecular cords, separated by a fine fibrovascular stroma. They commonly formed rosettes and pseudorosettes. Cells were moderately pleomorphic with round to ovoid nuclei and moderate amounts of eosinophilic cytoplasm. Nuclei had finely stippled chromatin and indistinct nucleoli and occasional megalokaryosis and binucleated cells were observed. Focal areas of necrosis were randomly distributed through the section. Neoplastic cells had antigen-specific labeling for somatostatin. There was also rare, focal to multifocal labeling for synaptophysin. Neoplastic cells were negative for PGP9.5, NSE, chromogranin A+B, insulin, glucagon, gastrin, PPP, endorphin and VIP. A morphologic diagnosis of gastric somastotatinoma with hepatic metastases was made.

Neoplasms with neuroendocrine differentiation occur throughout the gastrointestinal tract of humans and less frequently animals. Presumably they originate from the widely distributed cells comprising the dispersed neuroendocrine system and are classified as well-differentiated tumors (formerly "carcinoids"), neuroendocrine carcinomas, poorly differentiated neuroendocrine carcinomas, and mixed endocrine/exocrine carcinomas. Based on their hormone secretion, these neoplasms may be nonfunctional, secrete a single product, or be multihormonal. This bearded dragon neoplasm was classified as neuroendocrine carcinoma histologically and as a malignant somatostatinoma functionally. In humans, two clinical syndromes have been associated with somatostatinomas. The somatostatin syndrome is characterized by diabetes mellitus, cholelithiasis, weight loss, diarrhea, and anemia, and is frequently associated with pancreatic somatostatinoma. A second syndrome associated with somatostatinomas is von Recklinghausen's disease (RD, Neurofibromatosis type I), characterized by café-au-lait spots and multiple cutaneous neurofibromas. This syndrome is caused by a mutation in the NF-1 gene resulting in a lack of functional neurofibromin, a negative regulator of the Ras-related G proteins. In contrast to tumors associated with the somatostatin syndrome, somatostatinomas associated with RD are frequently of duodenal origin. In contrast to humans, somatostatinomas in bearded dragons appear to be primarily of gastric origin, but similar to their human pancreatic counterpart, exhibit widespread metastases and may be associated with a clinical syndrome of hypersomatostatinemia. The cause for the bearded dragon's apparent predisposition to this neoplasm is unknown. Somatostatinoma should be considered in the differential for animals presenting with anorexia, weight loss, and anemia, particularly if there is concurrent, otherwise unexplained, hyperglycemia.

References:

1. Kiupel M et al.: Histological Classification of Tumors of the Endocrine System of Domestic Animals, ed. Schulman FY, 2nd series (XII), pp. 49-68. AFIP, Washington, DC, 2008. **2**. Ritter J et al.: Gastric neuroendocrine carcinomas in bearded dragons (*Pogona vitticeps*). Vet Pathol, 2009. [Epub ahead of print]. **3.** Modlin IM et al.: Current status of gastrointestinal carcinoids. Gastroenterology, 128: 1717-51, 2005.

Muscular *Sarcocystis* in a South American Rattlesnake (*Crotalus durissus terrificus*)

***John Roberts**, Jaime Weisman, James Wellehan, E. Marie Rush, David Lindsay*

Alabama Dept of Agriculture and Industries, Thompson-Bishop-Sparks State Diagnostic Lab, Auburn, AL (Roberts); College of Veterinary Medicine (Weisman) and College of Wildlife/Environmental Institute, Auburn University, Auburn AL (Rush); College of Veterinary Medicine, University of Florida, Gainesville, FL (Wellehan), Virginia-Maryland Regional College of Veterinary Medicine, Vir***ginia*** Polytechnic Institute and State University, Blacksburg, VI (Lindsay)

An illegally imported, adult, female South American rattlesnake (*Crotalus dirissus terrificus*) was confiscated by wildlife officers, became moribund and died in their custody. At necropsy the fresh thawed carcass was moderately autolyzed with sufficient celomic adipose tissue but generalized muscle atrophy. The colon was distended with putrid digesta proximal to an obstructive colonic adenocarcinoma. Microscopically, skeletal muscle from head and three locations adjacent to vertebra demonstrated abundant sarcocysts measuring 0.1-0.5 by 0.05-0.15 mm encased in a thin wall. Sarcocysts were not identified in cardiac muscle and an inflammatory reaction associated with affected skeletal muscles was not observed. The sarcocysts greatly expanded the sarcoplasm of approximately 30 to 40 % of myocytes in all sampled locations. The primary sarcocyst wall was thin, generally measuring less than 2-µm thick. The interior of the sarcocyst was divided into many, variably sized and shaped compartments by 1-µm thick septa. Within these compartments were numerous eosinophilic, 2-3 µm in diameter, globular parasites. Transmission electron microscopy demonstrated sarcocystis metrocytes and bradyzoites with an electron-dense parasitophorous membrane that folded inward. PCR identified a species of *Sarcocystis* most closely related to *Sarcocystis mucosa*. This snake appears to be an intermediate host for a previously undescribed species of muscular Sarcocystis.

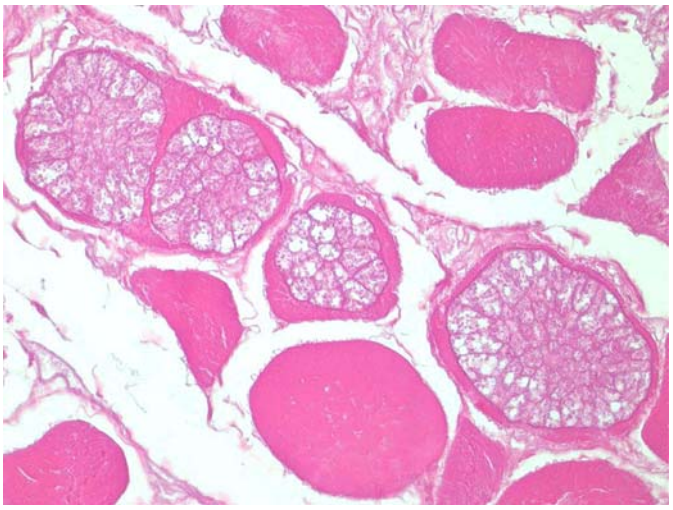

Ocular Mycobacteriosis in a Red-bellied Piranha (*Pygocentrus nattereri)*

Molly M. Evely *and Alan T. Loynachan*
University of Kentucky, Livestock Disease Diagnostic Center, Lexington, KY

The fresh water Red-bellied piranha (*Pygocentrus nattereri*) is naturally found in the Amazon River in Brazil. These fish can grow to a length of 33 cm, a weight of 3.5 kg and they have a reputation for being one of the most ferocious freshwater fish in the world. Despite their fearsome reputations they have become a common addition to both private and commercial aquariums.

Multiple fish in a privately owned and non-commercial aquarium had a week long duration of clinical signs that included: exophthalmos, tail and fin rot, eventual loss of equilibrium and anorexia. Two other fish had previously died, and there was no response to treatment with broad spectrum antibiotics. Necropsy of one piranha was performed within one hour of euthanasia. Significant gross lesions were limited to mild bilateral exophthalmos. Representative tissue samples were immersed in 10% neutral buffered formalin, routinely processed, embedded in paraffin wax, sectioned at 5 μm, stained with H&E, and examined by light microscopy. Lung and liver were aerobically cultured on blood agar plates and significant bacteria were not isolated. The eye was cultured at room temperature on blood agar plates and Lowenstein-Jensen medium and an acid-fact bacterium was isolated. DNA sequence analysis of the 16s rRNA and rpoβ genes identified the organism as *Mycobacterium chelonae*.

Microscopically, the eye had multifocal granulomatous choroiditis, scleritis and episcleritis with intralesional acid-fast bacteria. The choroid and periocular connective tissue contain multifocal to coalescing, well demarcated granulomas ranging from 0.5-1.5 mm. Granulomas contain necrotic centers that occasionally contain mineral, and are surrounded by moderate numbers of epitheloid macrophages, lymphocytes and plasma cells, and fibroblasts. Low to high numbers of lymphocytes and macrophages infiltrate the periocular adipose and connective tissue, extend to the limbus and surround the optic nerve. To enhance visualization of organisms, the eye was stained with Kinyouns Acid-Fast and low numbers of acid-fast bacilli were present in macrophages within the granulomas.

Fish mycobacteriosis is a systemic, chronic, progressive and often fatal disease that is most likely capable of affecting all species of fish and is caused by several species of Mycobacterium; the most common of which is *Mycobacterium marinum*. *Mycobacterium fortuitum* has been less frequently documented and is most commonly seen in freshwater fish while *Mycobacterium chelonae* infections have primarily been identified in pacific cold water salmonid species. The mode of transmission has not been well established but ingestion of contaminated feed, cannibalism of infected fish, transovarian and direct transmission from water through dermal wounds have been suggested. Frogs, snakes, turtles and snails are potential reservoirs, and infection of aquarium fish may be due to contamination from the aquarium environment by algae, moss or decorative tree roots. The pathogenesis is poorly characterized. Clinical signs of fish tuberculosis are quite variable and may include: anorexia, emaciation, skin discoloration, scale loss, vertebral deformities and exophthalmia. Numerous variably sized granulomas may be present on any parenchymatous tissue throughout the body, but are especially common in the spleen, kidney, and liver. Numerous acid-fast bacteria are often observed within the granulomas. There is no well accepted treatment for these potentially zoonotic bacteria other than depopulation and facility disinfection.

Effects of *Clostridium perfringens* beta toxin on the rabbit small intestine

Francisco A. Uzal, *Juliann Saputo, Jackie Parker and Joaquin Ortega*
California Animal Health and Food Safety laboratory, UC-Davis

C. perfringens type C necrotic enteritis mainly affects newborns, but also adults of many species, including humans. This microorganism produces two major toxins, i.e., alpha and beta, the latter being responsible for most clinical signs and lesions of clostridial enteritis. Beta toxin is exquisitely sensitive to the action of trypsin, which explains why most cases of *C. perfringens* type C occur in newborn animals. The current slide is part of a study to evaluate the role of different toxin genes of *C. perfringens* type C in small intestinal loops of rabbits. A whole culture of a wild-type strain of this microorganism, mixed with trypsin inhibitor, was inoculated into a ligated ileal loop of a rabbit that was kept under anesthesia for 6 hrs. After this, the animal was euthanized, and the intestinal loop was collected and processed routinely for histology. The intestinal loop treated with *C. perfringens* type C (this slide) had severe diffuse necrotizing enteritis, characterized by complete loss of absorptive cells along the villi and coagulation necrosis of the lamina propria with abundant karyorrhectic debris. The villi had almost completely disappeared and were replaced by a series of low denuded bumps that were multifocally covered by a pseudomembrane of hemorrhage, neutrophils, necrotic enterocytes, cell debris and numerous Gram-positive bacteria. A few preserved crypts were observed focally, although most of the crypt epithelium was necrotic and sloughed. Thrombi were observed in some mucosal blood vessels. The submucosa was edematous and hyperemic; submucosal lymphatic vessels were distended with proteinaceous material and neutrophils. Fibrin thrombi were common in submucosal veins. The changes observed in the rabbit intestine are very acute and almost identical to those seen in natural cases of *C. perfringens* type C necrotic enteritis in other animal species.

Encephalitozoon causing infection in multiple puppies in a kennel

Gayle C. Johnson, *Robert S. Livingston*

Veterinary Medical Diagnostic Laboratory (Johnson) and Research Animal Diagnostic Laboratory (Livingston), College of Veterinary Medicine, University of Missouri, Columbia, MO

A breeder of Brussels Griffon dogs reported neurologic signs and eventual death in three 7-9 week old puppies from somewhat related different litters over a period of 2 months. Affected puppies were smaller than their littermates, anorectic and had difficulty ambulating and swallowing. The clinical course prior to euthanasia was around 7 days, during which force-feeding and antibiotic treatment had no ameliorating effect on the clinical signs of one puppy. Fixed tissues from 2 of the puppies were received for microscopic evaluation. The most severe histopathologic lesions were found in brain, and were characterized by multiple microglial and histiocytic nodules distributed throughout gray and white matter of the entire brain, which were associated with extensive neuronal loss, capillary endothelial hyperplasia, white matter degeneration and astrogliosis. Abundant to uncommon spore-containing pseudocysts were found in endothelial cells, macrophages and neuropil in the brain. Both inflammatory lesions and cysts were much more abundant in one puppy than in the other. Additional cysts were present in kidney (2/2), spleen (1/2), and heart (1/1) of the puppies. Both puppies also had hepatic lipidosis. Spores within the pseudocysts stained positively with Gram and acid fast stains, were negative when with Giemsa stain, and demonstrated punctate staining of the spores with PAS stain. The organisms were not detected by immunohistochemical techniques to detect *Neospora*, *Leishmania* or *Toxoplasma*, but did stain with reagents against *Sarcocystis neurona* and *Sarcocystis falcatula*. These staining results, combined with PCR testing identified the etiology as *Encephalitozoon cuniculi*,[i] a microsporidian. Three genotypes of *Encephalitozoon* are known to exist. Type III is thought able to maintain a life cycle in dogs[ii], and has been documented as a zoonosis of immunocompromised people. In foxes and possibly in dogs, prenatal infections are also thought possible. The mode of transmission was not established for this outbreak, but dog to dog transmission by subclinically infected shedders is credited with being able to maintain infection within non-kennel canine populations. Interestingly another recently presented case of canine encephalitozoonosis involved a Brussels Griffon puppy as well, suggesting either spread of infection between kennels or a breed susceptibility.[iii]

References:

[i] Wasson, K., Peper,R.L.: 2000, Mammalian microsporidiosis. Vet Pathol 37:113-128.
[ii] E.S. Didier, C.R. Vossbrinck, M.D. Baker, et al.: 1995, Identification and characterization of three *Encephalitozoon cuniculi* strains, Parasitol **111:** 411–421.
[iii] Hoane,J.S., Agnew,D.W., Snowden,K.F: 2008, Disseminated encephalitozoonosis in a dog. Abstr 168, Vet Pathol 44:774.